Open Access Articles

The effect of low dose ionizing radiation on homeostasis and functional integrity in an organotypic human skin model

The Faculty of Oregon State University has made this article openly available.
Please share how this access benefits you. Your story matters.

Citation	von Neubeck, C., Geniza, M. J., Kauer, P. M., Robinson, R. J., Chrisler, W. B., & Sowa, M. B. (2015). The effect of low dose ionizing radiation on homeostasis and functional integrity in an organotypic human skin model. Mutation Research/Fundamental and Molecular Mechanisms of Mutagenesis, 775, 10-18. doi:10.1016/j.mrfmmm.2015.03.003
DOI	10.1016/j.mrfmmm.2015.03.003
Publisher	Elsevier
Version	Version of Record
Terms of Use	http://cdss.library.oregonstate.edu/sa-termsofuse

Mutation Research 775 (2015) 10–18

Contents lists available at ScienceDirect

Mutation Research/Fundamental and Molecular Mechanisms of Mutagenesis

journal homepage: www.elsevier.com/locate/molmut
Community address: www.elsevier.com/locate/mutres

The effect of low dose ionizing radiation on homeostasis and functional integrity in an organotypic human skin model

Claere von Neubeck[a,b], Matthew J. Geniza[c], Paula M. Kauer[d], R. Joe Robinson[d], William B. Chrisler[d], Marianne B. Sowa[d,*]

[a] German Cancer Consortium (DKTK) partner site Dresden, OncoRay - National Center for Radiation Research in Oncology, Faculty of Medicine and University Hospital Carl Gustav Carus, Technische Universität Dresden, Fetscherstrasse 74, 01307 Dresden, Germany
[b] German Cancer Research Center (DKFZ), Im Neuenheimer Feld 280, 69120 Heidelberg, Germany
[c] Molecular and Cellular Biology Program, Oregon State University, Corvallis OR 97331, USA
[d] Health Impacts and Exposure Science, Pacific Northwest National Laboratory, Richland WA 99352, USA

ARTICLE INFO

Article history:
Received 18 November 2014
Received in revised form 10 February 2015
Accepted 3 March 2015
Available online 16 March 2015

Keywords:
3D skin equivalent
Differentiation profile
Ionizing radiation
Heavy ion
Radiation quality

ABSTRACT

Outside the protection of Earth's atmosphere, astronauts are exposed to low doses of high linear energy transfer (LET) radiation. Future NASA plans for deep space missions or a permanent settlement on the moon are limited by the health risks associated with space radiation exposures. There is a paucity of direct epidemiological data for low dose exposures to space radiation-relevant high LET ions. Health risk models are used to estimate the risk for such exposures, though these models are based on high dose experiments. There is increasing evidence, however, that low and high dose exposures result in different signaling events at the molecular level, and may involve different response mechanisms. Further, despite their low abundance, high LET particles have been identified as the major contributor to health risk during manned space flight. The human skin is exposed in every external radiation scenario, making it an ideal epithelial tissue model in which to study radiation induced effects. Here, we exposed an *in vitro* three dimensional (3-D) human organotypic skin tissue model to low doses of high LET oxygen (O), silicon (Si) and iron (Fe) ions. We measured proliferation and differentiation profiles in the skin tissue and examined the integrity of the skin's barrier function. We discuss the role of secondary particles in changing the proportion of cells receiving a radiation dose, emphasizing the possible impact on radiation-induced health issues in astronauts.

© 2015 Elsevier B.V. All rights reserved.

1. Introduction

Outside Earth's atmosphere, all astronauts will be exposed to space radiation, giving rise to NASA's concern with associated health risks. Current risk estimates for manned space flight are based predominantly on human epidemiological data following low linear energy transfer (LET) and high dose radiation exposures. However, space radiation is composed of high LET, low dose particle irradiation resulting in large uncertainties in health risk estimates. Although the average daily dose accumulated in space from particle irradiation is not high enough to cause acute radiation exposure health effects, several studies have demonstrated an increased cancer risk in animal models (summarized in [1]). Despite the relatively low abundance of high atomic number and energy (HZE) particles in space, they have an enhanced relative biological effectiveness (RBE) due in part to their high ionization potential [2,16] and pose and increased health risk relative to more abundant protons.

A three dimensional (3-D) human organotypic skin model was employed in this study. The choice of skin as an epithelial model is three-fold, (1) skin is a relatively radiation sensitive organ, (2) it will receive a radiation dose in all external exposure scenarios, and (3) it is easily biopsied for validation of results in the astronaut population. The ICRP has estimated a nominal risk coefficient (cancer cases/10,000 persons/Sv) for skin in a sex specific population of exposed 18–64 years olds [3]. The nominal risk coefficient for skin is 670 versus 116 for the second most sensitive tissue, the female breast (see Ref. [3] table A.4.19, page 210). This makes skin the most highly sensitive tissue to ionizing radiation exposures. However, ionizing radiation induced skin cancers are almost exclusively non-lethal basal cell carcinomas [4], thus accounting for its relatively low tissue weighting factor (~3) and the common belief skin is a "radio-resistant" tissue. The high sensitivity of radiation induced responses makes skin an excellent model for examining low dose

* Corresponding author. Tel.: +1 509 371 6898; fax: +1 509 371 7304.
E-mail address: marianne.sowa@pnnl.gov (M.B. Sowa).

http://dx.doi.org/10.1016/j.mrfmmm.2015.03.003
0027-5107/© 2015 Elsevier B.V. All rights reserved.

effects at a molecular level where the endpoint is not metastatic disease.

The human organotypic skin model is composed of fibroblasts expressing extracellular matrix proteins in the dermis, and keratinocytes in the fully developed epidermis. New epidermal cells are exclusively formed through mitosis in the stratum basale (basal layer) and move up though the strata spinosum, granulosum, and corneum as they differentiate. Keratinocytes reach terminal differentiation at the air interface and are converted into corneocytes. Disturbances to the homeostatic regulation of keratinocyte proliferation, differentiation and death leads can lead to skin diseases such as atopic dermatitis, psoriasis and ichthyosis [5,6]. The complex homeostasis of proliferation and differentiation is characterized by changes in protein expression that define cell phenotype. Keratin 10 (K10) expression is a marker for the spinous and the granular layers [7]. Filaggrin is a major component of both the cornified layer and the granular layer where it is expressed. The skin protects the body against pathogens as well as oxidative, chemical and mechanical stresses. Mutations in the filaggrin gene are associated with a variety of skin diseases with disrupted skin barrier function [8]. External factors that induce alterations in the homeostatic regulation such as space relevant ions [9], environmental toxins as well as chronic trauma and inflammation [10] can contribute to benign and malignant epidermal cell growth leading to the most frequent human cancer type, epidermal tumors [11].

Our central hypothesis is that low doses of HZE radiation are capable of disturbing the homeostatic regulation of epithelial development, resulting in an LET dependent alteration in the proliferation and differentiation profiles. To address this hypothesis, the total number of cells in the basal layer, their proliferative activity, and the overall area of viable and differentiating keratinocytes in the epidermis of a 3-D organotypic skin model post exposure to space relevant low doses of high LET radiation were measured. In addition, the spatial distribution of the differentiation markers K10 and filaggrin in tissue sections as well as the epidermal barrier function, a functional outcome, were evaluated. Our data will contribute to the improvement of health risk estimates for astronauts on deep space missions, and to the development of a mechanistic understanding of the effects of low dose, high LET radiation exposures in epithelial tissues.

2. Material and methods

2.1. Tissue culture and irradiation

In vitro 3-D organotypic skin model consisting of epidermal keratinocytes and dermal fibroblasts were obtained from MatTek (EpiDermFT 400, MatTek Corp., Ashland, MA, USA). Tissue samples were randomized upon receipt to exclude production specific alterations. Samples were grown at 37 °C, 95% humidity and 5% CO_2 in a 6-transwell insert system and maintained in 3 ml of maintenance medium (MatTek Corp.). Three hours prior to irradiation, the culture media was replaced with 2 ml fresh media. Due to constraints in beam time availability, sample age and equilibration times (minimum 24 h) could not be held constant. Ion exposures were performed at the NASA Space Radiation Laboratory (NSRL) at Brookhaven National Laboratory (BNL, Uptown, NY, USA, campaigns IIA, IIB and IIC). Table 1 summarizes the ion exposure conditions, including ion species, LET, energy, and dose. Exposures were designed to deliver either a mean value of one primary ion traversal/basal cell (F2 = 1.1×10^{-3} ions/μm^2) or one traversal for every third cell in the basal layer (F1 = 3.6×10^{-4} ions/μm^2) [12]. Neon information from previous experimental exposures is included for the purpose of discussion only [13]. Samples were oriented at 45° from the incident particle beam to provide a more

Table 1
Summary of ion exposure conditions employed at NSRL. Beam radii and the δ-ray mean hits per cell were determined using GERMCode [19]. Neon data included for discussion purposes only [12].

Ion	LET (keV/μm)	Energy (MeV/u)	Range (g/cm^2)	Fluence 1	Fluence 2	Beam radius (μm)		Fluence 1 (F1) 3.6×10^{-4} ions/μm^2		Fluence 2 (F2) 1.1×10^{-3} ions/μm^2	
								Mean hits/cell		Mean hits/cell	
				3.6×10^{-4} ions/μm^2	1.1×10^{-3} ions/μm^2						
				Dose (cGy)	Dose (cGy)	Core	Penumbra	Core	δ-rays > 0.1 cGy	Core	δ-rays > 0.1 cGy
O^{+8}	18	500	29.05	0.11	0.31	0.239	45	0.33	0.51	1	1.56
Ne^{+10}	35	300	10.23	0.2	0.6	0.205	63	0.33	0.62	1	1.88
Si^{+14}	60	400	11.69	0.35	1.06	0.248	73	0.33	0.71	1	2.16
Fe^{+26}	174	600	16.25	1	3	0.268	137	0.33	1.04	1	3.16

uniform irradiation to all samples and to minimize scattering and secondary ionizations from the container walls. Post exposure, the culture media of samples with an incubation time longer than 8 h was supplemented with an additional 1 ml of fresh media. Time matched controls are included for all exposures.

2.2. Proliferation

Cell proliferation was measured using the Click-iT® EdU Alexa Fluor® 488 Imaging Kit (Invitrogen Corporation, Carlsbad, CA, USA) following the manufacturer's protocol. EdU is a nucleoside analog of thymidine and is incorporated into DNA during synthesis and repair. After irradiation, samples were incubated in medium containing 0 or 40 μM EdU until fixation of tissue and medium was exchanged daily. After the staining, slides were dehydrated and coverslipped with cytoseal xyl (Thermo Fisher Scientific, Waltham, MA, USA). Fluorescent imaging was performed using constant settings on a Nikon eclipse TE 1300 microscope (Nikon, Melville, NY, USA) with motorized stage (Ludl, Hawthorne, NY, USA) and Qimaging Retiga 1300 or QICAM Fast 1394 camera (Qimaging, Surrey, Canada) controlled by Volocity (PerkinElmer, Waltham, MA, USA). In three imaged tissue sections, a minimum of ~1200 cells/section for the epidermis and of ~300 cells/section for the dermis were analyzed to determine total cell numbers and percentage of EdU positive cells.

2.3. Immunostaining and imaging

Samples were harvested, fixed in 4% paraformaldehyde, dehydrated, embedded in paraffin, and cut into 5 μm sections (microtome, Leica RM 2155, Buffalo Grove, IL, USA) for histological examination. For analysis of morphology, samples were deparaffinized and rehydrated, then stained using a standard hematoxylin and eosin (H&E staining) protocol as described in [14]. For protein expression, the antigen was unmasked by heating slides in 10 mmol/l citrate buffer for 10 min (pH 6.0, microwave). The slides were washed in deionized water and incubated in 1% H_2O_2 for 10 min to inactivate endogenous peroxidases. The samples were washed thrice in PBS and incubated with 3% BSA in PBS for 1 h to block nonspecific binding. Sections were incubated with the primary antibody overnight at 4 °C. Antibodies used and concentrations were: 2 μg/ml mouse anti-K10 (clone DE-K10, Thermo Fisher Scientific) and 4 μg/ml mouse anti-filaggrin (ab17808, Abcam, Cambridge, MA, USA). Antibody binding was detected with the LSAB™-HRP-DAB+ kit (DAB, Dako North America Inc. Carpinteria, CA, USA) following the manufacturer's protocol. The slides were counterstained with Harris hematoxylin (Thermo Fisher Scientific), dehydrated and coverslipped with cytoseal xyl (Thermo Fisher Scientific). Tissue sections were imaged using an Olympus BX 40 microscope (Olympus America Inc., Center Valley, PA, USA) and a moticam 2300, 3.0 M pixel camera controlled by Motic Images plus 2.0 software (Motic, Richmond, Canada). The images were 1280 pixels wide, corresponding to a calibrated width of 627 μm at 10-fold magnification. Regions of interest were defined using MetaMorph® Microscopy Automation & Image Analysis Software (Molecular Devices, CA, USA) and the mean areas of positively stained cells or of the viable epidermis were calculated with their corresponding standard errors of the mean (SEM). As the width of the image was held constant, observed changes correspond to changes in layer thickness. However, the thickness of a layer is not always constant over the width of a sample and quantitative data are therefore discussed as mean areas of five fields of view. The average number of basal cells was determined in 14 optical fields for K10 stained images, yielding ~650 cells at 1 h and ~450 cells at 120 h.

2.4. Barrier function

Tissues exposed to 3 cGy (F2) of Fe ions were assayed at various times post-exposure for skin barrier functionality. Lucifer yellow solution (1 mmol/l, fluorescent cytoplasm stain, Sigma Aldrich) was pipetted on the cornified layer and incubated for 2 h at 37 °C. Positive control data was obtained by disrupting the barrier by treating with 100 mmol/l sodium dodecyl sulfate (SDS, Sigma Aldrich) for 20 min prior to incubating with Lucifer yellow. Tissues were then fixed, embedded and sectioned as above. Slides were stained for 1 h with 1 μmol/l SYTO® 60 in PBS (red fluorescent nucleic acid stain, Molecular Probes/Life technologies, Carlsbad, CA USA). Imaging was done with a Zeiss LSM710 confocal laser-scanning microscope and images were processed with ZEN lite 2011 (both Carl Zeiss MicroImaging GmbH, Jena, Germany). Lucifer yellow and SYTO® 60 were laser excited with 405 nm and 610 nm, respectively. A total of six sections for two biological replicates per condition were analyzed. If no green fluorescence was observed in the viable epidermis or the dermis, the barrier was considered intact and functional.

2.5. Statistical analysis

All data are expressed as the mean ± SEM. Group differences were tested for statistical significance using a Student's t-test. A p-value less than 0.05 was considered statistically significant. See appropriate sections for sample replicates analyzed.

3. Results

In order to test the hypothesis that space radiation affects epithelial homeostasis in a radiation quality dependent manner, we measured proliferation and differentiation profiles in a human skin epithelial model. Exposures were designed to deliver either a mean value of one primary ion traversal/basal cell ($F2 = 1.1 \times 10^{-3}$ ions/μm^2) or one traversal for every third cell in the basal layer ($F1 = 3.6 \times 10^{-4}$ ions/μm^2) [12]. Time points were chosen to examine short term (<24 h) and longer term responses (≥24 h) where proliferating cells will have gone through one or more cell cycles. In the following sections, proliferation activity studies, followed by area measurements for the viable epidermis and the differentiated layers, will be presented as a function of increasing LET. Observations made in histological sections are correlated with barrier function measurements for Fe ion exposures. We note that we may refer to relative LET values used as lower (18 keV/μm), medium (60 keV/μm) and high (174 keV/μm). However, we stress that all exposure conditions to the energetic ions presented here are categorized as high LET exposures.

3.1. Characterization of tissue construct

The organotypic skin construct continues to differentiate and develop during its time in culture. Due to beam time allocations, tissue exposures cannot always be performed at the same relative sample age and detailed characterization of the tissue changes over time is necessary. Fig. 1A presents the relative sample age for the various ion exposures reported. The specific data collection points for each ion are represented by vertical hash marks. Fig. 1B und C presents the basal cell counts and changes in the average area of epidermal layers as a function of sample age in the absence of radiation, respectively. The number of basal cells decreases in the early samples, reaching a plateau after a relative sample age of four days (Fig. 1B). The skin tissue continues to differentiate as it ages with the overall thickness decreasing over time (Fig. 1C). As indicated by the small variability in the data at a given time point, samples are fairly uniform among different sample lots. Due to the dynamic nature of the skin tissue, results presented in the sections that follow are for

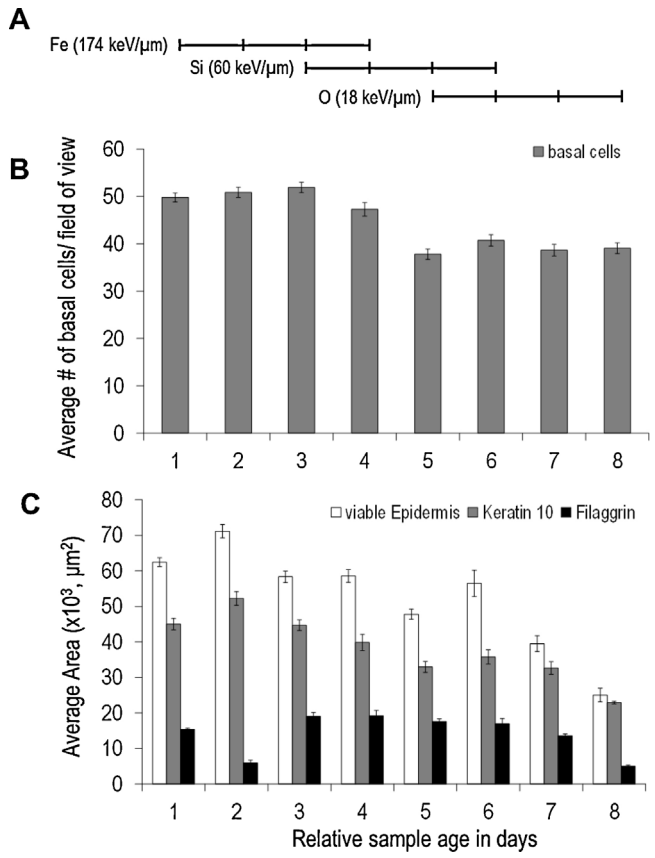

Fig. 1. Characterization of unexposed skin tissue as a function of time in culture. (A) Relative sample age in days for each exposure condition. Vertical bars indicate sample harvesting time points for a given ion exposure. (B) The average number of basal cells determined from Keratin 10 stained tissue sections. (C) Average area of viable epidermis (H&E, white bars) and the differentiation profile of Keratin 10 (gray bars) and Filaggrin (black bars) measured in DAB stained tissue sections. Original image magnification used in (B) and C) for outlining 10x (average = 21 ± SEM).

representative experiments with time matched controls. The data trends were verified in replicate experiments.

Fig. 2 shows representative images of tissue sections stained to define epidermal thickness (H&E staining, Fig. 2A), and differentiation profiles (K10, Fig. 2B and filaggrin, Fig. 2C) following exposure to Si ions. The images suggest a thinning of the viable epidermis over time as well as time- and fluence-dependent changes in the differentiation profiles. Similar staining patterns of basal cells, K10 and filaggrin are observed for O and Fe ion exposures. It should be noted that changes in the positively stained areas do not necessarily represent changes in the expression level of the individual cell; rather it indicates the fraction of tissue positively expressing the protein.

3.2. Proliferation

3.2.1. EdU-incorporation in S-phase cells

The proliferative activity of the skin tissue construct was measured as a function of time post exposure to O, Si and Fe ions (Fig. 3). Fig. 3A shows a representative Click-iT® EdU fluorescence image of DNA synthesizing cells in the skin construct. Nuclei have been counterstained with Hoechst 33342 to allow determination of total cell numbers present. Fig. 3B shows the percentage of cells actively proliferating in both the epidermis and dermis. In the epidermis, the amount of proliferation in sham irradiated tissues varies from 5–12% at 24 h reflecting relative sample age differences (see Fig. 1). Following ion exposure, changes in epidermal proliferation occur relative to control samples but with no clear pattern based on radiation quality (Fig. 3B). In O ion exposed samples, radiation appears to predominantly affect the early proliferative response. The proliferation activity is decreased significantly at 3 and 9 h post exposure to F2. However, exposure to F1 caused an increase in proliferation at 24 h post exposure. A similar fluence dependence is observed following Fe ion exposures with F1 enhancing proliferation and exposure to F2 reducing proliferation, however, the temporal profile is shifted to longer times (≥ 24 h). The temporal profile and fluence dependence for the Si ion exposures shows no clear trend, increasing proliferation at 3 h and 72 h for F1, and 3 h and 24 h for F2. A reduction in proliferating cells was only observed at 48 h post exposure to F1.

Data on time dependent radiation induced proliferative changes in the dermis are presented in the lower panels of Fig. 3B. A very small fraction of cells in the dermis are actively proliferating, making it difficult to detect significant changes following exposures. No significant changes were observed following O ion exposures. Si and Fe ions only produced significant alteration in proliferation at 48 and 24 h post exposure, respectively.

3.2.2. Basal cell counts

Basal keratinocytes are the only actively proliferating part of the epidermis; repopulating the basal layer and supplying the differentiated layers with post-mitotic cells. An increase or reduction in basal cell numbers is therefore associated with changes in the proliferation activity of the epidermal layer and changes in the kinetics of differentiation (see [13]). Fig. 4 shows the number of basal cells after O, Si and Fe ion exposures (Fig. 4A–C). The most significant radiation induced changes are observed following exposure to O ions. Exposure to both fluences resulted in an increase in basal cell numbers at 1, 3 and 9 h and a decrease at 24 h before the cell numbers return to control level at 72 h post exposure (Fig. 4A). In contrast to these findings, exposure to Si ions with F1 caused a decrease in cell number at 8 and 24 h post exposure, and exposure with F2 resulted in a decrease at 3, 8, and 24 h. Both samples treated with Si ions are above control levels at 72 h (Fig. 4B). Exposure to Fe ions (Fig. 4C) with F1 resulted in a decrease at 8 and 24 h post exposure. Treatment with F2 shows a decrease at 24 and 72 h. In sum, exposure to the lower LET ions (O) increases the basal cells numbers while exposure to intermediate and higher LET ions (Si and Fe) tend to reduce the basal cell numbers.

3.3. High LET exposure effects

Fig. 5 summarizes the area measurements for the viable epidermis (A–C) and the differentiation markers K10 (D–F) and filaggrin (G–I). The data for each of these endpoints are presented in separate sections.

3.3.1. Viable epidermis

Fig. 5(A–C) summarizes time and fluence dependent changes in the average area of the viable epidermis for skin tissue constructs exposed to O (Fig. 5A), Si (Fig. 5B), and Fe (Fig. 5C) ions. There is no general temporal trend in the data but there is an LET dependent response. For O ion exposures, there is evidence of an increase in thickness in all samples which is significant at 9 and 72 h (Fig. 5A). Increasing the LET to 60 keV/µm (Si ions, Fig. 5B) induced no short term changes but at time points ≥24 h a decrease in thickness is statistical significant. Very few significant changes are observed following Fe exposures (Fig. 5C). For all ions examined, changes in epidermal thickness appear to be fairly independent of fluence (dose), with no obvious trend observed.

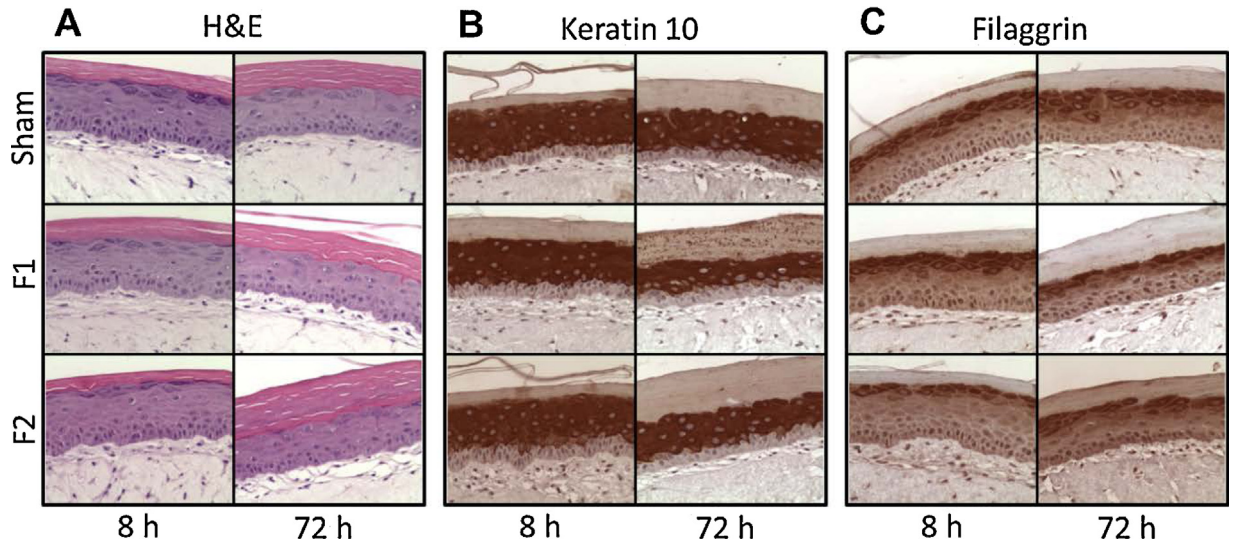

Fig. 2. Representative histological sections of the high LET radiation effects on tissue morphology and differentiation. Samples were exposed to 400 MeV/u Si ions and stained for (A) H&E, (B) Keratin 10 and (C) filaggrin. For Keratin 10 and filaggrin, positive DAB staining appears dark brown in the image. All tissues are counterstained with hematoxylin. F1 = 3.6×10^{-4} ion/μm^2, F2 = 1.1×10^{-3} ion/μm^2, Original image magnification 20x.

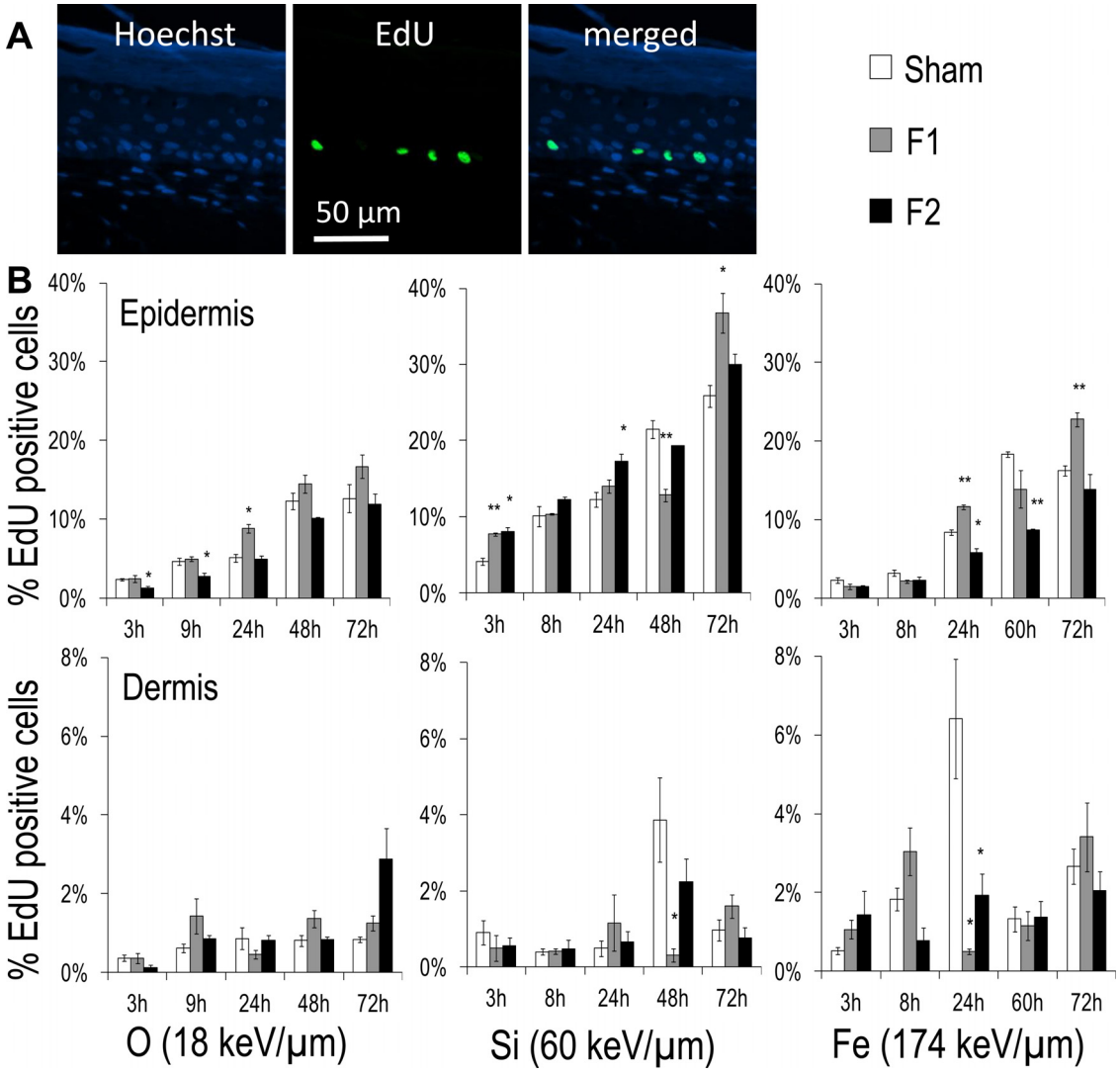

Fig. 3. High LET effects on proliferation as a function of time post exposure. (A) Representative tissue section of cells which have integrated EdU during DNA synthesis. Tissues were stained with EdU/Alexa 488 fluorescent coupled antibody (green) and DNA counterstaining with Hoechst 33342 (blue). (B) Mean percentage ± SEM of EdU positive nuclei per tissue section for epidermal keratinocytes and dermal fibroblasts as a function of time post exposure to 500 MeV/u O, 400 MeV/u Si and 600 MeV/u Fe ($n = 3$). Exposure fluences: F1 = 3.6×10^{-4} ion/μm^2, F2 = 1.1×10^{-3} ion/μm^2, Original image magnification used for scoring: 20x. * = p value < 0.05, ** = p value < 0.005.

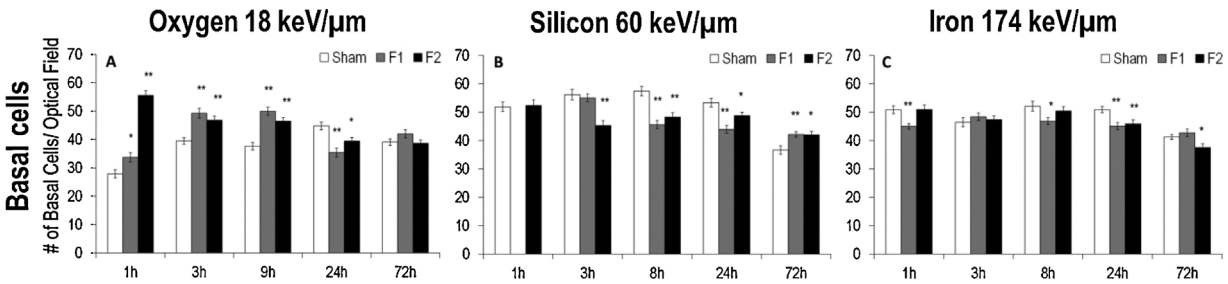

Fig. 4. High LET effects on basal cell counts as a function of time post exposure. The average number of basal cells in 14 optical fields was determined from Keratin 10 stained sections following exposure to (A) 500 MeV/u O, (B) 400 MeV/u Si and (C) 600 MeV/u Fe. Exposure fluences: F1 = 3.6×10^{-4} ion/µm^2, F2 = 1.1×10^{-3} ion/µm^2, * = p value < 0.05, ** = p value < 0.005. Original magnification used for scoring 10x. Gaps in data indicate sample loss.

3.3.2. *Differentiation profile*

Fig. 5(D–F) shows the average area of K10 positive epidermis representing the combined spinous and granular layers as a function of time post exposure. For O ions, there is evidence in the data towards increasing thickness where the lower fluence F1 results in a stronger response with an earlier onset relative to F2 exposed samples (Fig. 5D). Increasing the LET with Si ion (Fig. 5E) and Fe ion (Fig. 5F) exposures, changes the temporal pattern and regulation direction of the K10 positive areas. Si ion exposures cause an increase in K10 expression in the first 3 h, but later times show a significant decrease. However, the response is not constant for the two ion fluences measured. Fe ions show an increase at 8 and 72 h following F1 exposures, and a decrease at 3 h for F2.

Fig. 5(G–I) displays the changes in the average area of the granular layer (filaggrin positive area) as a function of time post exposure. The general trend at longer times is for a decrease in the filaggrin area with higher LET. Exposure to O ions (Fig. 5G) cause an increase in the filaggrin positive area at all time points (F1) and at 24 and 72 h (F2) post exposure. Exposure to Si ions (Fig. 5H) with F1 causes an increase at 3 and 8 h post exposure, and a decrease at 72 h post exposure. F2 enhances the positive stained areas only at 3 h while at 8 and 72 h the average area is below control levels. No statistically significant changes are observed for samples exposed to Fe ions at the lower fluence (Fig. 5I), and only minimal effects are observed for F2 exposures, with a decrease in area at 72 h.

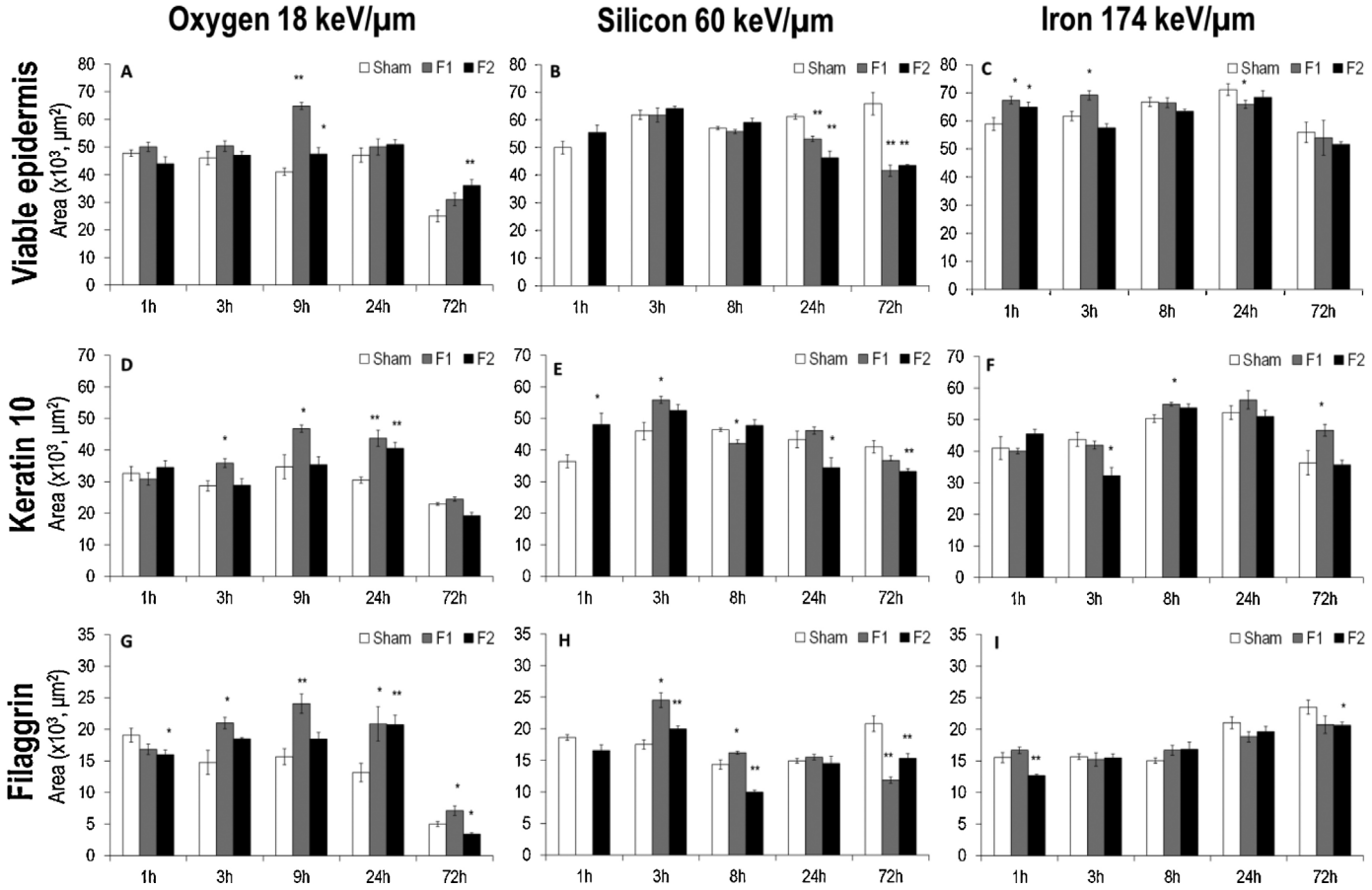

Fig. 5. High LET effects on the thickness of the viable epidermis (H&E, A-C), of the combined spinous and granular layers (Keratin 10, D–F) and on the granular layer (Filaggrin, G–I) following exposure to (A) 500 MeV/u O, (B) 400 MeV/u Si, and (C) 600 MeV/u Fe. Tissue sections ($n = 5 \pm$ SEM) were imaged (original image magnification 10x) and areas were outlined. Exposure fluences: F1 = 3.6×10^{-4} ion/µm^2, F2 = 1.1×10^{-3} ion/µm^2. * = p value < 0.05, ** = p value < 0.005. Gaps in data indicate sample loss.

3.3.3. Barrier function

Filaggrin, a major component in the cornified layer and of the skin barrier function [8], showed high LET radiation induced expression changes. To test the integrity of the skin barrier, samples were exposed to the highest dose and LET examined, Fe ions (F2), and evaluated at 8, 24, and 72 h post exposure. Fig. 6 shows representative confocal Images 8 h after exposure and the corresponding positive control. While SDS treatment resulted in Lucifer yellow leaking into the dermis, none of the radiation exposure conditions examined resulted in skin barrier breakdown (data not shown).

4. Discussion

In the event of long term deep space missions, one must address the question of how space radiation affects both the astronaut health during missions and upon return to Earth. NASA has identified low doses of high LET radiation as the major contributor to the astronauts' health risks in space, with cancer and cataract development, effects on the central nervous system and organ failure being the crucial concerns [2,15–17]. Few systematic studies have been performed on radiation quality effects following exposure to multiple ion species in complex model systems. Here, we studied the coordinated tissue response of a human 3-D organotypic epithelial model to low doses of high LET space relevant ion exposures in histological samples. Our goal is to develop a mechanistic understanding of skin homeostatic processes initiated and affected by low dose exposures of different radiation qualities. The acquired biological data, proliferation and differentiation profiles, are necessary for improvement of existing risk models, and to verify our own computational model on the effects of heavy ion radiation on epidermal homeostasis [13].

4.1. Physical considerations for radiation quality studies

Biological experiments with different HZE particles at constant fluences (particle/area) allow data interpretation based on track structure and beam features such as the contribution of δ-rays (Table 1). At low fluences, very few cells will be directly traversed by a particle receiving a relatively high dose, while neighboring non-traversed cells may receive a dose of essentially zero due to the heterogeneous energy deposition pattern of HZE particles [18,19]. There are approximately 1.1×10^{-3} cells/μm^2 in the basal layer of the 3-D organotypic model employed in this study [13]. These are the only actively dividing cells in the epidermis and therefore a likely biological target for radiation effects discussed here. The two ion fluences used correspond to a direct primary ion traversal in every basal cell (F2) or every third basal cell (F1). The traversals are stochastic events governed by Poisson statistics which is independent of particle type, energy and LET and strictly depend on fluence and numbers of target cells. Table 1 lists the mean hits per cell at both fluences. The Poisson distribution underestimates the exposed target volume due to disregard of contributions from secondary interactions or particle fragmentation. The Galactic Cosmic Ray Event-based Risk Model (GERM)-code [20] was used to estimate the beam radius and the contribution of δ-rays to the delivered dose (Table 1). Over the experimental range, the radii of the ion track cores are essentially constant and ion fragmentation was found to be negligible for the exposure geometry used. However, the production of secondary ions (δ-rays) leads to increased radii of the beam penumbras by a factor of three as the LET and Z increase (Table 1). The δ-rays contribute to the mean number of traversals/cell leading to an additional dose to the skin tissue affecting the biological response and the data interpretation. How aspects of the physical properties of the radiation field affect the proliferation and differentiation profiles in skin are addressed in the sections which follow.

4.2. Radiation quality effects

Cell proliferation and differentiation in the epidermis is a tightly regulated process. The data presented here show that exposure to low doses of high LET radiation induced changes in proliferation (Figs. 3 and 4) accompanied with alterations in the differentiation process (Fig. 5) but ultimately not to a compromised barrier function of the 3-D organotypic skin model (Fig. 6). However, the observed cellular interactions post exposures to high LET ions are complex both in their temporal and LET dependent responses. Here we found that the LET appears to be more important in determining the response than the dose delivered. The summarized general trend in our data indicates (i) for O ions (LET = 18 keV/μm) increased basal cell numbers and corresponding thickening of all epidermal layers, (ii) for Si ions (LET = 60 keV/μm) a reduction of basal cells and a thinning of all epidermal layer and (iii) for Fe ions (LET = 174 keV/μm) reduced basal cell numbers but only modest changes in the epidermal layers. Studies with human skin fibroblasts [21,22] and keratinocytes [23] found quantitative and qualitative differences in cellular response post exposure to various ions. In particular, the increased contribution of secondary particles e.g. δ-rays was discussed [24,25] underlining the importance of LET dependent responses.

Indications for a disturbance in proliferation and differentiation homeostasis are the radiation-induced alterations in basal cell numbers and thickness of the viable epidermis relative to the unexposed controls. Extensive experimental studies on the epidermal tissue regeneration response post exposure to fractioned photon radiotherapy reveal three central mechanisms: loss of asymmetric stem cell division, acceleration of stem cell proliferation and abortive division of epidermal cells [26–29]. To the best of our knowledge there are no experimental studies which asses the epidermal tissue regeneration responses post exposure to space relevant HZE ions. Nonetheless, it seems very likely that the regenerative mechanisms can be applied to particle exposed skin tissue. For epidermal skin, no widely accepted marker yet exists that allow for the specific identification of epidermal stem cells. Therefore, only the proliferation kinetics of the entire cell population can be assessed with the 3-D organotypic skin model.

It was been suggested that radiation induces accelerated repopulation in squamous epithelia [30]. The majority of cells damaged by radiation will undergo a limited number of abortive divisions resulting in near-normal differentiated daughter cells which counteract radiation-induced cell loss [30]. For a human skin model consisting of keratinocytes alone, enhanced proliferation activity in the basal layer was reported at 48 h and 72 h post exposure to 10 cGy low LET protons and a lack of a continuous basal layer at 72 h post exposure to 250 cGy of protons [31]. Similarly, in the results presented in this study, we found fluence dependent effects on basal cell numbers post exposure to low doses of high LET O, Si and Fe ions and corresponding changes in the thickness of the viable epidermis. The alterations observed persisted for 72 h implying a sustained disturbance of normal tissue homeostasis.

In this study, proliferation was measured by measuring basal cell kinetics and through EdU nucleoside analog incorporation. The comparison between the two assays reveals low overlap in regulation direction (Figs. 3 and 4) which is due to the different cell populations being monitored. EdU labeling captures mainly S-phase cells but also cells which repair radiation induced DNA damage while the number of basal cells represents changes in total cell numbers and can depend on kinetic changes induced in the differentiation profile [13]. For a mechanistic understanding of radiation-induced accelerated repopulation, total basal cell

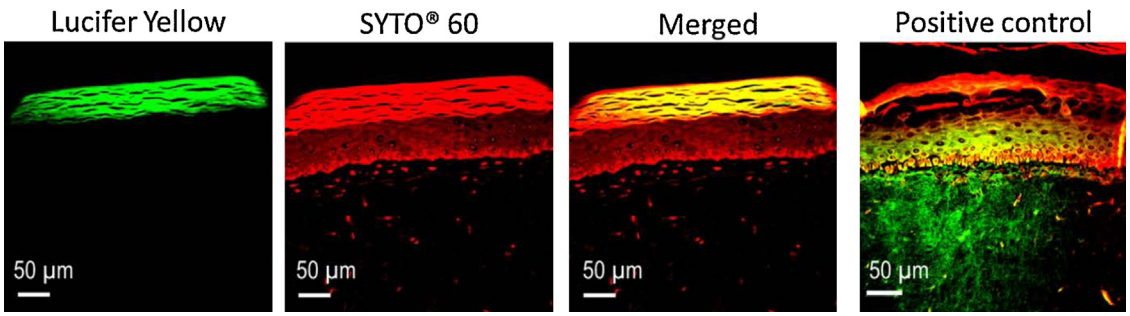

Fig. 6. The effect of high LET radiation on skin barrier function. Representative images of 600 MeV/u Fe ion exposed (LET = 174 keV/µm, F2 = $1.1*10^{-3}$ ion/μm^2) tissues section 8 h post exposure. Tissues were incubated with Lucifer yellow and counterstained with SYTO® 60. The unexposed positive control was incubated with 100 mM SDS for 20 min prior to Lucifer yellow addition. Original image magnification 20x.

numbers seem to be more important than EdU incorporation, representing both DNA repair and active proliferation. The apparently opposing effects observed in EdU labeling as a function of experimental condition (i.e. Fe ion fluence dependence at 24 h, Fig. 3B) might be explained by activation of cell cycle checkpoints. It is well known that the radiation-induced DNA damage response can limit entry into S-phase by activating cell cycle checkpoints. The full activation of the sensitive G1/S-Phase checkpoint is a relatively slow process, taking between 4 and 6 h, with the duration of the arrest increasing with applied dose [32]. The observation that some exposed samples yield more EdU positive cells at a lower fluence (dose) could be the result of a slower activation or a shorter duration of the G1/S-phase checkpoint in samples exposed to Fe ions of F1. However, a detailed study of cell cycle distributions in the basal layer would be needed to validate this supposition.

In a previous publication, exposure to Ne ions induced rapid, but transient effects on both cell proliferation and differentiation in the epidermis ([13], see Table 1 for beam details). Alternate hypotheses regarding radiation effects were evaluated by using an agent based model, and histology and qRT-PCR validated the modeling results. The recent model-based analysis of the effects of Ne exposures provides a template to understand the complex temporal responses of multicellular systems, and can be adapted to other epithelial tissues and ion species. The model allows us to integrate heterogeneous data such as cell numbers or thickness measurement to obtain insight about the specific cell-level processes that are altered by radiation of different quality. Given the complex time and fluence dependent changes in proliferation and differentiation markers observed here, modeling will likely play a key role in revealing the repopulation mechanisms underlying the observed radiation quality effects. Ongoing work extends the analysis of the data collected as part of the current study.

4.3. *Effects on barrier function*

In human skin, post-mitotic cells express structural proteins which form the physical barrier to the environment [33]. Filaggrin is a major component of the stratum corneum and is involved in keratin-filaggrin aggregation [34]. Mutations in the filaggrin gene are associated with a variety of skin diseases involving disrupted skin barrier function [9]. Abnormalities in the stratum corneum are often a secondary cause of altered proliferation [35]. In filaggrin knock-down experiments with an organotypic skin model it was shown that the stratum corneum maintained normal morphology but showed a disturbed barrier function in a dye penetration assay [34]. Low dose low LET exposures have been demonstrated to alter filaggrin processing in the human skin construct and a breakdown in the skin barrier has been proposed as a functional consequence [36]. Although LET dependent changes in the proliferation and differentiation profiles were observed in this study, neither morphological alterations in the stratum corneum in exposed or unexposed samples (Fig. 2) nor breakdown of the skin barrier following exposure to Fe ions (Fig. 6) were detected. Fractionated radiotherapy has been shown to be capable of disrupting the skin barrier in patients with radiation dermatitis [33]. However, excessive physical stress including a large radiation dose of 30 Gy (X-rays) to a stratum corneum model failed to induce any permanent change in the skin barrier [35]. These results suggest that a fractionated, high cumulative dose is necessary to disrupt the skin barrier with low LET X-rays. Although space radiation exposures occur in a protracted manner and the rare events of a high HZE particle traversal could be consider fractioned radiation, it appears unlikely that low doses of high LET radiation would be sufficient to cause a sustained disruption to the skin barrier function.

5. Conclusion

There is limited data available for the effect of HZE particles on human health. This study provides a comprehensive look at the effect of high LET ion exposures on skin homeostasis. From the data presented, it is obvious that the regulation of the closely linked processes of proliferation and differentiation is complex. However, the systematic collection of data in realistic tissue models provides a means of parameterizing and developing predictive models as has been shown previously [13], representing an expanding frontier in health risk predictions.

Conflicts of Interest

The author acknowledges there are no conflicts of interest.

Author Contribution

CVN planning of research, performing of experiments, data analysis, writing of manuscript.

MJG imaging, scoring and analysis of area data.

PMK performing experiments at NSRL, imaging, scoring and analysis of EdU data.

RJR performing experiments at NSRL, histological methods and preparations.

WBC imaging barrier function data.

MBS project idea and overall experimental design, planned the research, performed the experiments, data analysis, writing of manuscript.

Funding

This work was supported by the National Aeronautics and Space Administration [NNX10AB06G]; and the Biological and

Environmental Research Program (BER), U. S. Department of Energy [DE-AC06-76RLO].

Acknowledgments

We acknowledge the help and support of the Brookhaven National Laboratory NASA NSRL beam line operators, Drs. A. Rusek and M. Sivertz, and the medical department support staff, particularly our run coordinators, Dr. P. Guida, Ms. L. Thompson and Ms. A. Kim. We also acknowledge Ms. A. Schwartz, Ms. M. Burnet and Mr. J. Mendoza for assistance with experiments and data scoring, Mr. J. Pirkkanen, Mr. D. Mullen for manuscript preparation and Drs. A. L. Brooks and W. F. Morgan for critical manuscript review and discussion.

References

[1] E.L. Alpen, et al., Fluence-based relative biological effectiveness for charged particle carcinogenesis in mouse Harderian gland, Adv. Space Res. 14 (10) (1994) 573–581.
[2] F.A. Cucinotta, M. Durante, Cancer risk from exposure to galactic cosmic rays: implications for space exploration by human beings, Lancet Oncol. 7 (5) (2006) 431–435.
[3] ICRP, The 2007 Recommendations of the International Commission on Radiological Protection, in Publication 103, J. Valentin, Editor 2007.
[4] R.E. Shore, Radiation-induced skin cancer in humans, Med. Pediatr. Oncol. 36 (5) (2001) 549–554.
[5] S. Hoffjan, S. Stemmler, On the role of the epidermal differentiation complex in ichthyosis vulgaris, atopic dermatitis and psoriasis, Br. J. Dermatol. 157 (3) (2007) 441–449.
[6] C.N. Palmer, et al., Common loss-of-function variants of the epidermal barrier protein filaggrin are a major predisposing factor for atopic dermatitis, Nat. Genet. 38 (4) (2006) 441–446.
[7] N. Pasquariello, et al., Regulation of gene transcription and keratinocyte differentiation by anandamide, Vitam. Horm. 81 (2009) 441–467.
[8] H. Kawasaki, et al., Loss-of-function mutations within the filaggrin gene and atopic dermatitis, Curr. Probl. Dermatol. 41 (2011) 35–46.
[9] R. Masse, RBE for carcinogenesis following exposure to high LET radiation, Radiat. Environ. Biophys. 34 (4) (1995) 223–227.
[10] T. Batinac, et al., Apoptosis in skin cancer development and regression, Coll. Antropol. 31 (Suppl 1) (2007) 23–28.
[11] C. Lorz, C. Segrelles, J.M. Paramio, On the origin of epidermal cancers, Curr. Mol. Med. 9 (3) (2009) 353–364.
[12] J.H. Miller, et al., Confocal microscopy for modeling electron microbeam irradiation of skin, Radiat. Environ. Biophys. 50 (3) (2011) 365–369.
[13] C. von Neubeck, et al., Integrated experimental and computational approach to understand the effects of heavy ion radiation on skin homeostasis, Integr. Biol. (Camb) 5 (10) (2013) 1229–1243.
[14] Brown, H.S., Hematoxylin & Eosin (The Routine Stain)., 2002, Sigma–Aldrich H&H Informational Primer. 1-3.
[15] F.A. Cucinotta, et al., Space radiation cancer risks and uncertainties for Mars missions, Radiat. Res. 156 (5 Pt 2) (2001) 682–688.
[16] Cucinotta, F.A.K., M.H.;Chappell, L. J, Space Radiation Cancer Risk Projections and Uncertainties – 2010, 2011. NASA.
[17] W. Schimmerling, F.A. Cucinotta, J.W. Wilson, Radiation risk and human space exploration, Adv. Space Res. 31 (1) (2003) 27–34.
[18] International, C.o.R.U.a.M., Quantification and Reporting of Low-Dose and other Heterogeneous Exposures, 2011. Nuclear Technology Publishing, Ashford. p. v.
[19] F.A. Cucinotta, et al., Radiation dosimetry and biophysical models of space radiation effects, Gravit. Space Biol. Bull. 16 (2) (2003) 11–18.
[20] F.A. Cucinotta, et al., Nuclear interactions in heavy ion transport and event-based risk models, Radiat. Prot. Dosimetry 143 (2–4) (2011) 384–390.
[21] C. Tsuruoka, M. Suzuki, K. Fujitaka, LET and ion-species dependence for mutation induction and mutation spectrum on hprt locus in normal human fibroblasts, Biol. Sci. Space 18 (3) (2004) 188–189.
[22] C. Tsuruoka, et al., LET and ion species dependence for cell killing in normal human skin fibroblasts, Radiat. Res. 163 (5) (2005) 494–500.
[23] F. Wu, R. Zhang, F.J. Burns, Gene expression and cell cycle arrest in a rat keratinocyte line exposed to 56Fe ions, J. Radiat. Res. 48 (2) (2007) 163–170.
[24] T.-H. Yang, et al., Chromosomal changes in cultured human epithelial cells transformed by low- and high-LET radiation, Adv. Space Res. 12 (2–3) (1992) 127–136.
[25] E.A. Lebel, et al., Analyses of the secondary particle radiation and the DNA damage it causes to human keratinocytes, J. Radiat. Res. 52 (6) (2011) 685–693.
[26] I. Turesson, et al., Normal tissue response to low doses of radiotherapy assessed by molecular markers–a study of skin in patients treated for prostate cancer, Acta Oncol. 40 (8) (2001) 941–951.
[27] W. Dorr, Modulation of repopulation processes in oral mucosa. experimental results, Int. J. Radiat. Biol. 79 (7) (2003) 531–537.
[28] K. Liu, M. Kasper, K.R. Trott, Changes in keratinocyte differentiation during accelerated repopulation of the irradiated mouse epidermis, Int. J. Radiat. Biol. 69 (6) (1996) 763–769.
[29] A. Shirazi, K. Liu, K.R. Trott, Epidermal morphology, cell proliferation and repopulation in mouse skin during daily fractionated irradiation, Int. J. Radiat. Biol. 68 (2) (1995) 215–221.
[30] W. Dorr, H. Emmendorfer, M. Weber-Frisch, Tissue kinetics in mouse tongue mucosa during daily fractionated radiotherapy, Cell Prolif. 29 (9) (1996) 495–504.
[31] A. Mezentsev, S.A. Amundson, Global gene expression responses to low- or high-dose radiation in a human three-dimensional tissue model, Radiat. Res. 175 (6) (2011) 677–688.
[32] D. Deckbar, P.A. Jeggo, M. Lobrich, Understanding the limitations of radiation-induced cell cycle checkpoints, Crit. Rev. Biochem. Mol. Biol. 46 (4) (2011) 271–283.
[33] M. Schmuth, et al., Permeability barrier function of skin exposed to ionizing radiation, Arch. Dermatol. 137 (8) (2001) 1019–1023.
[34] M. Mildner, et al., Knockdown of filaggrin impairs diffusion barrier function and increases UV sensitivity in a human skin model, J. Invest. Dermatol. 130 (9) (2010) 2286–2294.
[35] H. Tagami, et al., Environmental effects on the functions of the stratum corneum, J. Investig. Dermatol. Symp. Proc. 6 (1) (2001) 87–94.
[36] F. Yang, et al., Quantitative phosphoproteomics identifies filaggrin and other targets of ionizing radiation in a human skin model, Exp. Dermatol. 21 (5) (2012) 352–357.